

## Electrochemical Characterization of Ordered Mesoporous Carbon Screen- Printed Electrodes

Daniel Martín-Yerga<sup>Z</sup>, Estefanía Costa Rama and  
Agustín Costa-García

Nanobioanalysis Group, Department of Physical and Analytical  
Chemistry, University of Oviedo, Oviedo 33006, Spain

« Previous | Next Article »  
Table of Contents

### This Article

doi:  
10.1149/2.0871605j  
es  
J. Electrochem. Soc.,  
2016 volume 163,  
issue 5, B176-B179

» Abstract

Figure Only

This is a preprint manuscript. Please, download the final and much nicer version at:

<https://doi.org/10.1149/2.0871605jes>

1  
2  
3  
4  
5  
6  
7  
8  
9  
10  
11  
12  
13  
14  
15  
16  
17  
18  
19  
20  
21  
22  
23  
24  
25

**Electrochemical characterization of ordered mesoporous carbon screen-  
printed electrodes**

*Daniel Martín-Yerga\*, Estefanía Costa Rama, Agustín Costa-García*

**Nanobioanalysis group**

Department of Physical and Analytical Chemistry

University of Oviedo

\* Corresponding author: Daniel Martín-Yerga

Department of Physical and Analytical Chemistry

University of Oviedo

8 Julián Clavería St., Oviedo 33006 (Spain)

E-mail: martindaniel@uniovi.es

Telephone: (+34) 985103486

26 **ABSTRACT**

27

28 Screen-printed electrodes have become an essential tool in the development of  
29 electrochemical sensors and biosensors. Among the materials used for the fabrication, the  
30 most employed are the different forms of carbon. In this work, the electrochemical  
31 characterization of ordered mesoporous carbon screen-printed electrodes is carried out. The  
32 results show that the surface area is enhanced and the resistance to the electron transfer is  
33 highly reduced in comparison to graphite screen-printed electrodes. Although a lower limit of  
34 detection is obtained for screen-printed graphite, ordered mesoporous carbon electrodes  
35 showed a better voltammetric selectivity.

36

37

38

39

40

41

42

43

44

45

46

47

48

49

50

## 51 INTRODUCTION

52 Carbon materials are widely used in electrochemical applications due to its good electrical  
53 properties, low cost, and acceptable chemical inertness. Several kinds of carbon have been  
54 used in electrodes such as graphite paste, glassy carbon or highly ordered pyrolytic graphite  
55 (HOPG). In recent years, with the rise of the nanotechnology, novel carbon nanomaterials  
56 such as carbon nanotubes, carbon black or graphene, have appeared providing different  
57 electrode properties. Among the carbon materials employed in electrochemistry is ordered  
58 mesoporous carbon (OMC). OMC have a large surface area, ordered mesostructure with well-  
59 defined and controlled pore size, chemical inertness and high thermal stability<sup>1</sup>. OMC has  
60 been employed as electrode material for electroanalytical applications<sup>2,3</sup>, protein  
61 immobilization<sup>4</sup>, and biosensors<sup>5</sup>.

62

63 Screen-printed electrodes are a very promising tool for point-of-care (POC) testing<sup>6,7</sup>. They  
64 have ideal characteristics such as small size, low cost, ease of use and portability. For these  
65 reasons, the use of screen-printed electrodes modified with ordered mesoporous carbon could  
66 lead to substantial improvements in the field of (bio)sensing. However, although there are  
67 several published studies using conventional electrodes as mentioned previously, the literature  
68 using SPEs modified with OMC is scarce. For instance, they have been employed for  
69 glucose<sup>5</sup> or norepinephrine<sup>8</sup> detection. The complex modification of the surface with OMC  
70 reported in these works is an important disadvantage for the preparation of simple  
71 electrochemical sensors. In contrast, the use of commercial readily available electrodes can  
72 avoid the tedious steps of the surface modification. Therefore, the characterization of  
73 commercial OMC screen-printed electrodes (OMCSPEs) may provide some useful  
74 information about their potential as readily available sensing transducers.

75

76 In this work, we carried out the electrochemical characterization of ordered mesoporous  
77 carbon screen-printed electrodes by cyclic voltammetry using two model species such as  
78 ferrocyanide and dopamine, and, also by electrochemical impedance spectroscopy. A critical  
79 comparison between the electrochemical properties obtained for OMCSPEs and for screen-  
80 printed graphite electrodes is presented. Furthermore, the analytical performance for the  
81 dopamine determination and the selectivity towards other species such as uric acid and  
82 ascorbic acid were evaluated.

83

## 84 **EXPERIMENTAL**

### 85 Materials and instrumentation.

86 Potassium ferrocyanide, potassium ferricyanide, dopamine hydrochloride and potassium  
87 chloride were purchased from Sigma-Aldrich. Sodium hydroxide and phosphoric acid were  
88 purchased from Merck. Ultrapure water obtained with a Millipore Direct Q5 purification  
89 system from Merck-Millipore was used throughout this work. Electrochemical measurements  
90 were carried out with an Autolab PGSTAT12 (Metrohm) potentiostat/galvanostat interfaced  
91 to a computer system and controlled by Autolab GPES 4.9 software for voltammetric  
92 measurements and by Autolab FRA 4.9 software for electrochemical impedance spectroscopy  
93 (EIS) measurements.

94 Commercial ordered mesoporous carbon (OMCSPEs) and screen-printed graphite electrodes  
95 (SPCEs) were purchased from DropSens (ref. 110OMC and 110, respectively). All indicated  
96 potentials are related to the silver quasireference screen-printed electrode. All measurements  
97 were performed at room temperature by adding 40  $\mu$ l of the specific solution to the  
98 electrochemical cell. Working solutions of ferrocyanide and dopamine were prepared in KCl  
99 0.1 M. A JEOL 6610LV scanning electron microscope was used to imaging the working  
100 electrodes.

101 Electrochemical measurements

102 For ferrocyanide, cyclic voltammetry was performed from -0.2 to +0.5 V. For dopamine,  
103 cyclic voltammetry was performed from 0 to +0.7 V (+0.9 for SPCEs). Potential step was 4  
104 mV for both cases, and CV was performed at different scan rates such as 10, 25, 50, 75, 100,  
105 250 and 500 mV/s.

106 Electrochemical impedance spectroscopy (EIS) was performed with a  $[\text{Fe}(\text{CN})_6]^{3-/4-}$  solution  
107 (5 mM) prepared in 0.1 M KCl. A potential of +0.12 V and an AC amplitude of 10 mV were  
108 applied. The impedance data was fitted to the Randles equivalent circuit.

109 Dopamine chronoamperometric measurements were performed by applying a potential of  
110 +0.5 V to OMCSPEs and +0.7 V to SPCEs for 50 s.

111

112 **RESULTS AND DISCUSSION**

113 The microscopic characterization of OMCSPEs was carried out by scanning electron  
114 microscopy (SEM) (Figure 1). For comparison, the graphitic surface of SPCEs was also  
115 analyzed. For SPCEs, a very rough surface with a continuous-like structure of nanoparticles is  
116 observed. This structure is probably due to the graphitic powder and binder used for the  
117 fabrication of these electrodes. For OMCSPEs, a different surface is observed with some kind  
118 of microtubes (up to 200 nm in diameter) and several layers, which lead to a very porous  
119 three-dimensional structure. However, the structure is quite heterogeneous and different  
120 surface features can be observed.

121

122 The surface of the OMCSPEs was characterized by electrochemical impedance spectroscopy  
123 and a comparison was carried out with screen-printed graphite electrodes. Figure 2 shows the  
124 impedance spectra in the form of a Nyquist plot, and the equivalent circuit used to fit the EIS  
125 data is shown in the inset, where  $R_s$  is the solution resistance,  $R_{ct}$  is the charge transfer

126 resistance,  $C_{dl}$  is the double-layer capacitance, and  $W$  is the Warburg impedance. For SPCEs  
127 (circles curve), the impedimetric response observed is characteristic of the equivalent circuit  
128 used with a semicircle at high frequencies and a straight line at low frequencies. For  
129 OMCSPEs (triangles curve), the behaviour is closer to an ideal conductor, with a semicircle  
130 of a very small diameter at high frequencies indicating that the electron transfer in this kind of  
131 electrodes is significantly enhanced in comparison to SPCEs. The values obtained after the  
132 fitting of the EIS data for  $R_{ct}$  were  $380 \pm 52$  and  $32 \pm 4 \Omega$  for SPCEs and OMCSPEs,  
133 respectively. Furthermore, a significant difference was also estimated for  $C_{dl}$ , obtaining  
134 values of  $1.07 \pm 0.02$  and  $34 \pm 5 \mu\text{F}/\text{cm}^2$  for SPCEs and OMCSPEs, respectively. These  
135 values indicate a much higher capacitance of the electrode surface in OMCSPEs compared to  
136 SPCEs, probably due to the three-dimensional structure able to store a higher amount of  
137 charge between layers.

138

139 A comparison between the electrochemical response of SPCEs and OMCSPEs using two  
140 model analytes (ferrocyanide and dopamine) by cyclic voltammetry was carried out. Cyclic  
141 voltammograms at different scan rates of a solution of  $0.5 \text{ mM}$  of  $[\text{Fe}(\text{CN})_6]^{4-}$  in  $0.1 \text{ M KCl}$   
142 were recorded on SPCEs and OMCSPEs. Figure 3A shows the voltammograms for  
143 OMCSPEs. The different electrochemical response for both electrodes at  $50 \text{ mV/s}$  is shown in  
144 the Figure 3B. The peak potential difference ( $\Delta E_p$ ) was  $76 \text{ mV}$  for OMCSPEs and  $124 \text{ mV}$   
145 for SPCEs. The  $\Delta E_p$  value closer to the theoretical reversibility ( $59 \text{ mV}$ ) for OMCSPEs  
146 indicates an improvement in the electron transfer in good agreement with the EIS data.  
147 Although a similar behaviour is found for both electrodes, a study to evaluate the rate-limiting  
148 step of the electrochemical reaction was carried out. Peak currents (anodic and cathodic) were  
149 plotted against the scan rate and the root of the scan rate. For both cases, a linear plot was  
150 obtained, indicating that the rate-limiting control is the diffusion of the species to the

151 electrode surface, and the Randles-Sevcik equation for a diffusion-controlled process can be  
152 applied:

$$153 \quad i_p = (2.69 \times 10^5) n^{3/2} A C D^{1/2} v^{1/2}$$

154 where  $i_p$  is the peak current intensity (A),  $n$  is the number of electrons transferred in the  
155 electrochemical reaction,  $A$  is the electrode area ( $\text{cm}^2$ ),  $C$  is the bulk concentration of the  
156 analyte ( $\text{mol}/\text{cm}^3$ ),  $D$  is the diffusion coefficient of the analyte ( $7.26 \times 10^{-6} \text{ cm}^2/\text{s}$  as found in  
157 the literature<sup>9</sup>), and  $v$  is the scan rate ( $\text{V}/\text{s}$ ).

158 Using this equation, the electroactive area for both electrodes was calculated, obtaining values  
159 of  $0.072 \pm 0.003 \text{ cm}^2$  and  $0.082 \pm 0.003 \text{ cm}^2$  for SPCEs and OMCSPEs, respectively. The  
160 porous OMC surface result in an increased area compared to SPCEs. However, these values  
161 are well below the geometric area of the electrode even with the rough surface of both  
162 electrodes. This fact can mainly be due to the binder and other impurities present in the  
163 structure preventing the electron transfer.

164

165 The standard heterogeneous rate constant,  $k^0$ , was estimated using the Nicholson method<sup>10</sup>  
166 where the peak separation potential ( $\Delta E_p$ ) is correlated to a dimensionless function ( $\psi$ ) and  
167 this function is used to calculate the rate constant using the following equation:

$$168 \quad \psi = k^0 (D_O/D_R)^{\alpha/2} (RT)^{1/2} (\pi n F D v)^{-1/2}$$

169 where  $D_O$  and  $D_R$  are the diffusion coefficient for the redox couple species ( $\text{cm}^2/\text{s}$ ),  $\alpha$  is the  
170 transfer coefficient (0.5),  $R$  is the universal gas constant ( $\text{J}/\text{mol K}$ ),  $T$  is the absolute  
171 temperature (K),  $n$  is the number of electrons transferred,  $F$  is the Faraday constant ( $\text{C}/\text{mol}$ )  
172 and  $v$  is the scan rate ( $\text{V}/\text{s}$ ).

173 In order to estimate the  $\psi$  function, the following equation developed by Swaddle et al.<sup>11</sup> can  
174 be employed:

$$175 \quad \ln \psi = 3.69 - 1.16 \ln(\Delta E_p - 59)$$



176

177 Using this methodology, the  $k^0$  for  $[\text{Fe}(\text{CN})_6]^{4-}$  at both electrodes was estimated, obtaining  
178 values of  $1.5 (\pm 0.6) \times 10^{-3}$  and  $3.3 (\pm 0.6) \times 10^{-2}$  for SPCEs and OMCSPEs, respectively. This  
179 increment indicates a much faster electron transfer at OMCSPEs, reaching a value very close  
180 to the theoretically reversible for one electron transfer. Besides the best features presented by  
181 the OMC respect to graphite, the electrode surface seems to be covered with a lower amount  
182 of binder, and as previously reported in the literature<sup>12</sup>, it could have a great impact on the  
183 electron transfer rate.

184

185 The electrochemical behaviour on SPCEs and OMCSPEs of a more complex system,  
186 dopamine, was also evaluated. Cyclic voltammograms at different scan rates of a solution of  
187 0.5 mM of dopamine in 0.1 M KCl were recorded at SPCEs and OMCSPEs. Figure 3C shows  
188 the voltammograms at different scan rates for OMCSPEs and Figure 3D shows the  
189 electrochemical response at 100 mV/s for a SPCE and OMCSPE. As in the  $[\text{Fe}(\text{CN})_6]^{4-}$  case,  
190 the  $\Delta E_p$  decreased significantly at OMCSPEs compared to SPCEs. For dopamine, the effect is  
191 greater, and the  $\Delta E_p$  decreased from 552 mV at SPCEs to 76 mV at OMCSPEs, indicating a  
192 more reversible electrochemical reaction due to an enhanced electron transfer. In this case, a  
193 notable increment of the peak current is also observed for cathodic and anodic processes. The  
194 study of the rate-limiting step of the electrochemical reaction showed that both processes  
195 were diffusion-controlled (peak currents linearly proportional to the square root of the scan  
196 rate). Although dopamine appears to undergo adsorption on other carbon materials such as  
197 nanotubes<sup>13</sup>, it does not seem to occur on OMCSPEs, where only a diffusional process is  
198 observed. Therefore, the increment of the peak current is due mainly to the increased surface  
199 area involved in the electron transfer and a decreased resistance to charge transfer, and not to  
200 any adsorption process.

201

202 Using the Nicholson method, the  $k^o$  for dopamine at both electrodes was estimated, obtaining  
203 values of  $1.2 (\pm 0.8) \times 10^{-4}$  and  $1.53 (\pm 0.05) \times 10^{-3}$  for SPCEs and OMCSPEs, respectively. A  
204 significant increment of the electron transfer rate is also observed for dopamine at OMCSPEs.  
205 This fact makes OMCSPEs a good alternative for a diffusion-controlled detection of different  
206 species, which undergo adsorption on other advanced carbon materials such as nanotubes or  
207 graphene.

208

209 In order to evaluate the analytical behaviour of dopamine in these two types of electrodes,  
210 chronoamperometric measurements for different concentrations of dopamine were carried out  
211 using SPCEs and OMCSPEs. Square-wave or differential-pulse voltammetries seem like most  
212 appropriate techniques for dopamine detection, however, the initial results with these  
213 techniques showed a lower reproducibility for OMCSPEs than using chronoamperometry. For  
214 the chronoamperometric detection for OMCSPEs, a potential of +0.5 V was chosen, while  
215 that for SPCEs, +0.7 V was the optimal potential. As expected for the improvement of the  
216 electron transfer, a lower detection potential can be used to carry out the oxidation of  
217 dopamine, which is positive for the analytical selectivity using such electrodes. In the Figure  
218 4, the calibration plots obtained for both electrodes are presented. For OMCSPEs, a linear  
219 range from 50 to 2000  $\mu\text{M}$  was obtained, while that for SPCEs it was from 5 to 2000  $\mu\text{M}$ .  
220 These results seem to make clear as the difference in the capacitive current contribution may  
221 be responsible for being unable to observe signals at low dopamine concentrations in  
222 OMCSPEs, since the background current is much higher, and therefore, the minimum  
223 detectable concentration is lower for SPCEs.

224

225 The simultaneous detection of several species whose oxidation potential is near the oxidation  
226 of dopamine such as ascorbic acid and uric acid is a constant concern, and different types of  
227 electrodes have been employed<sup>14,15</sup>. In this case, a proof of concept was conducted to compare  
228 the voltammetric response of these species in both SPCEs and OMCSPEs using a 0.1 M pH 7  
229 PBS buffer. Linear sweep voltammograms of different solutions of these species (separately  
230 and mixtures of species) at concentrations of 0.4 mM for ascorbic acid, and 0.2 mM for uric  
231 acid and dopamine, were recorded. Figure 5 shows the voltammetric response of a solution  
232 with the three species. At SPCEs, two broad unresolved peaks are observed, and therefore, the  
233 species could not be determined simultaneously. After evaluating the individual responses, it  
234 was observed that the dopamine and ascorbic acid appeared at the same potential, while that  
235 the uric acid is the species at the more positive potential. For OMCSPEs, a better resolution of  
236 the three species is obtained as they appear at different potentials, from most negative to  
237 positive potentials: ascorbic acid, uric acid and dopamine. This fact seems to be a very  
238 important advantage of OMCSPEs over SPCEs, and it is direct consequence of the  
239 improvement in the electron transfer between the ordered mesoporous carbon and the  
240 electroactive species.

241

## 242 **CONCLUSIONS**

243 Commercial ordered mesoporous carbon screen-printed electrodes have shown interesting  
244 electrochemical characteristics such as an enhanced electron transfer even for simple analytes  
245 as ferrocyanide and dopamine. The porous structure of OMC leads to an increment of the  
246 electrode surface area, enhancing the electrochemical response and may prove useful for  
247 modification with biomaterials in biosensing applications. As a drawback, OMC shows large  
248 double-layer capacitances, which could hinder small analytical signals, and therefore, they are  
249 not the best tool for ultrasensitive determinations. However, the enhanced electron transfer

250 leads to an improvement in the selectivity compared to graphite electrodes. The results of this  
251 work indicate that the OMCSPEs could be useful for some sensing applications where the  
252 limit of detection is not the critical aspect. Furthermore, OMCSPEs may prove interesting as  
253 solid-contact ion selective electrodes in potentiometric sensors for its high capacitance.

254

#### 255 **ACKNOWLEDGMENTS**

256 This work has been supported by the FC-15-GRUPIN-021 project from the Asturias Regional  
257 Government. Daniel Martín-Yerga thanks the Spanish Ministry of Economy and  
258 Competitiveness for the award of a FPI grant (BES-2012-054408).

259

#### 260 **NOTES**

261 The authors declare no competing financial interest.

262

263 **REFERENCES**

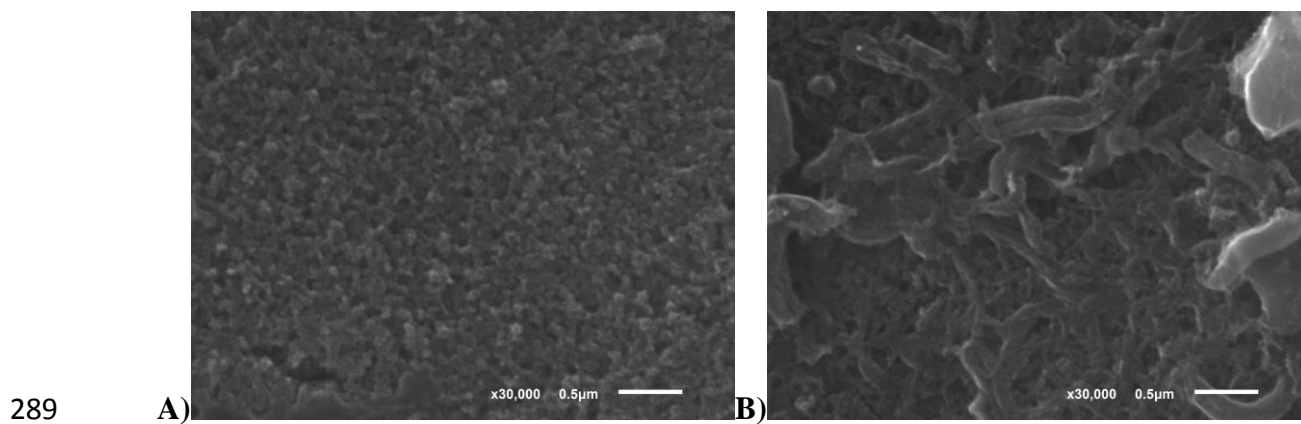
- 264 1. Z. Zhou and M. Hartmann, *Chem. Soc. Rev.*, **42**, 3894 (2013).
- 265 2. J. C. Ndamanisha, J. Bai, B. Qi, and L. Guo, *Anal. Biochem.*, **386**, 79–84 (2009).
- 266 3. J. C. Ndamanisha and L. Guo, *Anal. Chim. Acta*, **747**, 19–28 (2012).
- 267 4. E. Ghasemi, E. Shams, and N. Farzin Nejad, *J. Electroanal. Chem.*, **752**, 60–67 (2015).
- 268 5. M. Dai, S. Maxwell, B. D. Vogt, and J. T. La Belle, *Anal. Chim. Acta*, **738**, 27–34 (2012).
- 269 6. P. Fanjul-Bolado, D. Hernández-Santos, P. J. Lamas-Ardisana, A. Martín-Pernía, and A.  
270 Costa-García, *Electrochim. Acta*, **53**, 3635–3642 (2007).
- 271 7. Z. Taleat, A. Khoshroo, and M. Mazloum-Ardakani, *Microchim. Acta*, **181**, 865–891  
272 (2014).
- 273 8. M. Dai, B. Haselwood, B. D. Vogt, and J. T. LaBelle, *Anal. Chim. Acta*, **788**, 32–38  
274 (2013).
- 275 9. S. J. Konopka and B. McDuffie, *Anal. Chem.*, **42**, 1741–1746 (1970).
- 276 10. R. S. Nicholson, *Anal. Chem.*, **37**, 1351–1355 (1965).
- 277 11. T. W. Swaddle, *Chem. Rev.*, **105**, 2573–608 (2005).
- 278 12. N. A. Choudry, D. K. Kampouris, R. O. Kadara, and C. E. Banks, *Electrochem. commun.*,  
279 **12**, 6–9 (2010).
- 280 13. C. B. Jacobs, I. N. Ivanov, M. D. Nguyen, A. G. Zestos, and B. J. Venton, *Anal. Chem.*,  
281 **86**, 5721–5727 (2014).
- 282 14. D. Han, T. Han, C. Shan, A. Ivaska, and L. Niu, *Electroanalysis*, **22**, 2001–2008 (2010).
- 283 15. J. Ping, J. Wu, Y. Wang, and Y. Ying, *Biosens. Bioelectron.*, **34**, 70–6 (2012).
- 284

285 **FIGURES**

286

287 **Figure 1.** SEM micrograph of a screen-printed graphite electrode (**A**) and of a screen-printed

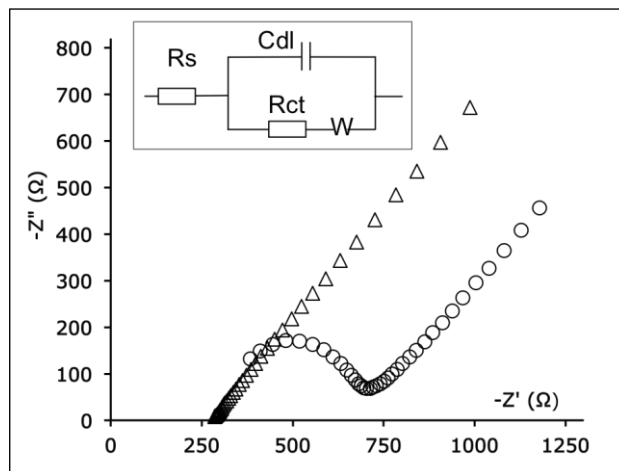
288 ordered mesoporous carbon electrode (**B**).



290 **Figure 2.** EIS data obtained for a SPCE (circles) and for an OMCSPE (triangles). Inset:

291 Randles equivalent circuit used for fitting the EIS data.

292

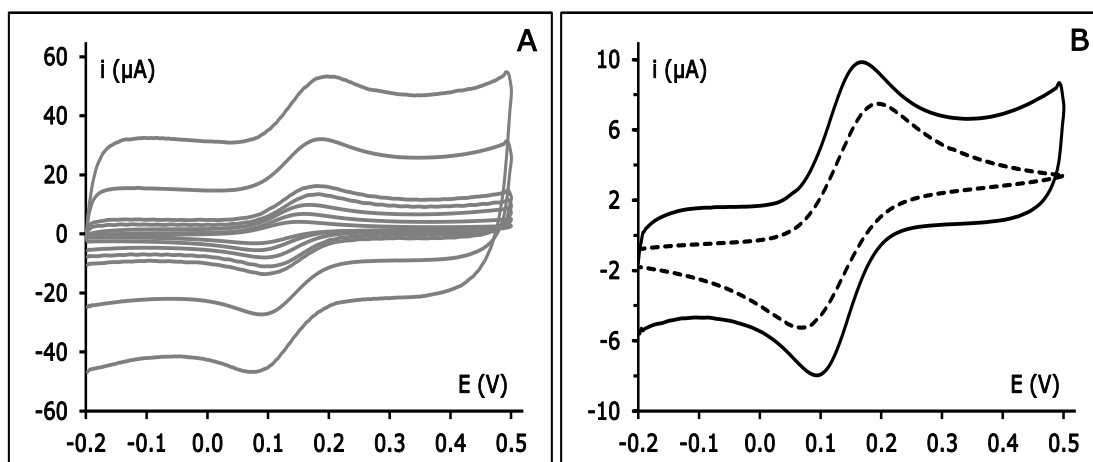


293

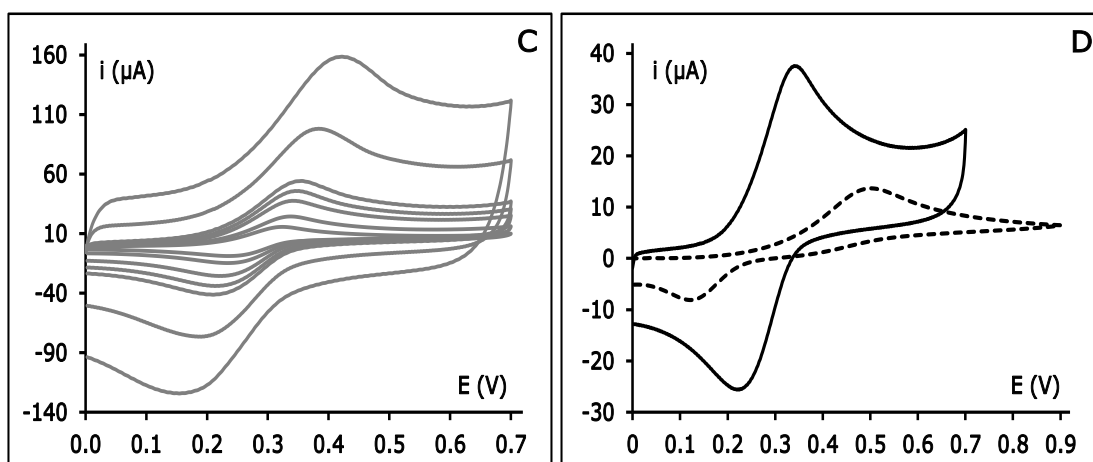
294 **Figure 3. A)** Cyclic voltammograms of 0.5 mM  $[\text{Fe}(\text{CN})_6]^{4-}$  at an OMCSPE using different  
295 scan rates. **B)** Cyclic voltammograms of 0.5 mM  $[\text{Fe}(\text{CN})_6]^{4-}$  at a SPCE (dashed line) and at  
296 an OMCSPE (solid line) using a scan rate of 50 mV/s. **C)** Cyclic voltammograms of 0.5 mM  
297 dopamine at an OMCSPE using different scan rates. **D)** Cyclic voltammograms of 0.5 mM  
298 dopamine at a SPCE (dashed line) and at an OMCSPE (solid line) using a scan rate of 50  
299 mV/s.

300

301



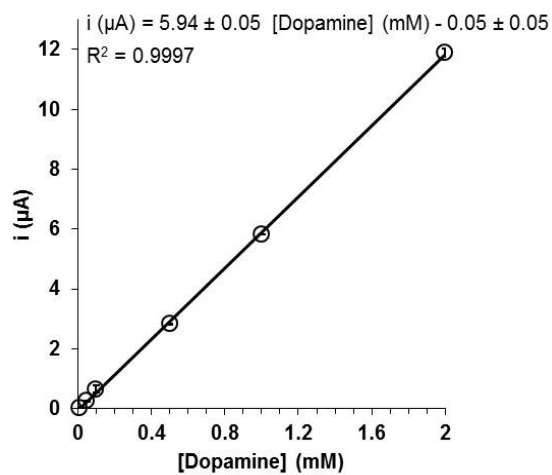
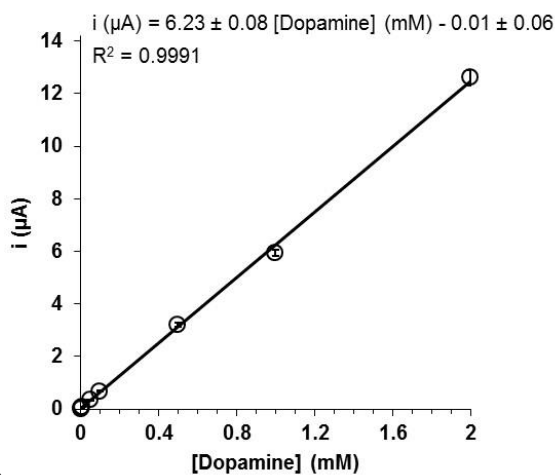
302





303 **Figure 4.** Calibration plots for dopamine using SPCEs (A) and OMCSPEs (B) by  
304 chronoamperometric measurements applying a potential of +0.7 V for SPCEs and +0.5 V for  
305 OMCSPEs during 50 s.

306



307 A)

307 B)

308

309

310

311

312

313

314

315

316

317

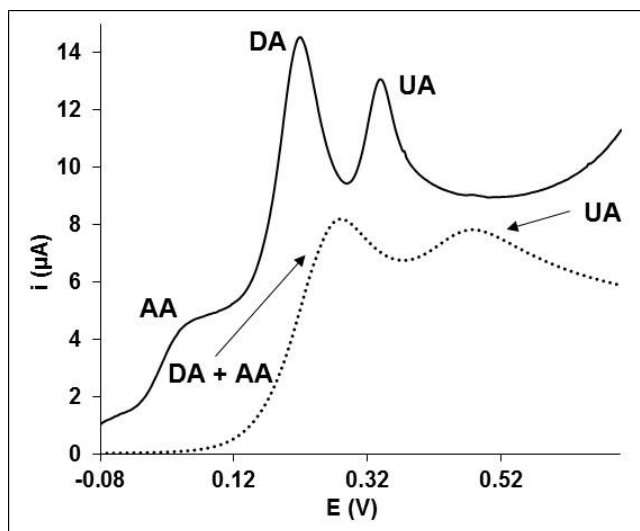
318

319

320

321 **Figure 5.** Linear sweep voltammograms for 0.4 mM ascorbic acid (AA) and 0.2 mM  
322 dopamine (DA) and uric acid (UA) in 0.1 M PBS pH 7 using a SPCE (dotted line) and a  
323 OMCSPE (solid line).

324



325